29th Congress of the International Council of the Aeronautical Sciences
St. Petersburg, Russia; September 7-12, 2014

ARTIFICIAL TURBULIZATION OF THE SUPERSONIC BOUNDARY LAYER BY DIELECTRIC BARRIER DISCHARGE

P.A. Polivanov, A.A. Sidorenko & A.A. Maslov
Khristianovich Institute of Theoretical and Applied Mechanics SB RAS
630090, Institutskaya, 4/1, Novosibirsk, Russia
polivanov@itam.nsc.ru

Keywords: *flow control, compressible boundary layer, transition, DBD*

Abstract

The most evident way to decrease drag and pollution of transonic airplanes is extensive using of laminar flow wherever it is possible. Unfortunately the laminar flows are difficult to implement in presence of adverse pressure gradients caused by the shock wave / boundary layer interaction. Undesirable flow separation may eliminate all advantages of the laminar flow. Therefore it is necessary to design a technique of fast and reliable turbulization of the boundary layer right upstream of the interaction zone to reduce the separation. The paper is devoted to experimental and numerical study of plasma application for turbulization of the boundary layers at M=1.5, 2. The experiments demonstrated the possibility of the supersonic boundary layer turbulization by the dielectric barrier discharge. Parametric study of this effect was performed by CFD to find the mechanisms of the turbulization and optimize plasma discharge parameters.

1 Introduction

Ecological demands and increasing price of fuel cause an intensive study of laminar flow wing problem. It is generally acknowledged that transonic and supersonic commercial airplanes of the next generations will be equipped with a laminar wing [1] to decrease the viscous drag. Unfortunately the laminar boundary layer has weak resistance to adverse pressure gradients especially ones produced by shock waves. The shock waves are the native feature of the transonic and supersonic flow around complex bodies and their interaction with the boundary layer is of great importance. It is well known (see, for example [2]) that the separation of the laminar boundary layer on the transonic airfoil has bigger extent in comparison with turbulent separation resulting in the total drag increasing. Elimination of this negative effect with keeping all advantages of the laminar flow is possible if the laminar-turbulent transition is forced right upstream of the shock wave. The shock waves usually move due to variation of the flow parameters, angle of attack and etc. therefore the point of turbulization has to move correspondingly. The traditional turbulators such as roughness and vanes are fixed to the wing surface therefore some controllable devices are needed [3].

The number of papers dealing with active methods of laminar-turbulent transition control at supersonic speeds is not much. Most often studies are connected with the effect of roughness [4]. But the interest in active control method is growing. For example in the paper [5] steady and unsteady blowing jets generating a turbulent boundary layer at Mach number M = 4.6 were considered. In this paper the possibility to use the jets for the flow turbulization was successfully demonstrated. However it was obtained that the position of the transition is significantly far downstream from the point of introduction of the perturbation, which reduces the usefulness of this technology in practice. Furthermore this technique requires a significant modifications of the aircraft structure.

The plasma actuator based on the dielectric barrier discharge (DBD) is a popular device for flow control. Dielectric barrier discharge (DBD) is very easy to integrate into the surface. This actuator has a complex influence on the flow by the ionic wind and discharge streamers and allows to turbulize the flow. The main advantage of DBD (in comparison with other discharge) is low energy consumption that allows to use it during the whole flight. At the moment main part of study was done for subsonic speeds. The evidence of the possibility of using DBD for turbulization of boundary layer (BL) in supersonic flows was not demonstrated. Indirectly, the possibility of using DBD for turbulization of BL has been shown in [6]. In this experimental paper, authors studied the parameters of the transonic flow in wake of airfoil at high angles of attack. It has been shown that pulsations in wake significantly decreases when the discharge was on. Reynolds number in these experiments was considerably low allowing to suggest that the BL on the airfoil was laminar and discharge led to turbulization the flow, which reduced the flow separation.

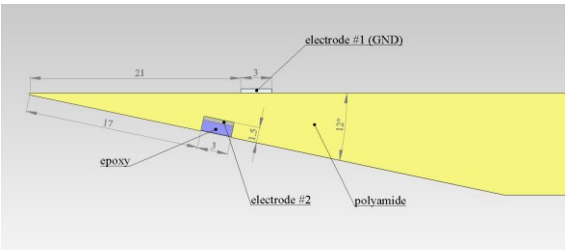

Fig. 1. . Scheme of DBD


Fig. 2. Experimental model

It is necessary to note the study [7] which shows the possibility of using DBD to control of turbulent separated flow in compression corner at Mach number M = 4.7. It gives hope that DBD can be used for high-speed flows. But the results of [7] only qualitative and therefore require quantitative verification.
Unfortunately in the experiment is rather difficult to control of some discharge parameters. This makes difficult to understand the mechanisms of the discharge effect on the flow. Therefore, the general goal of this work is to perform parametric numerical study of the discharge effect on a laminar BL.

2 Experimental and numerical setup

The experiments has been performed in wind tunnel T-325 for Mach number $M_\infty = 2$, and freestream unit Reynolds number $Re_1 = 10 \cdot 10^6$ m^{-1}. The experimental model for was a plexiglas or steel flat plate with sharp leading edge. The plasma actuator was installed in the replaceable polyamide nose section (Fig. 1) or glass insert in other cases. The sandpaper turbulator was placed 70 mm downstream of the plasma actuator to obtain the turbulent boundary on the model if plasma is off.

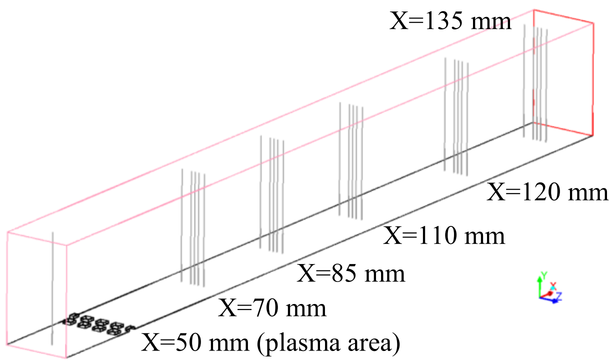

Fig. 3. Schematic of computational domain

DBD consisted from two electrodes separated by layer of dielectric. The first electrode was exposed to surrounding gas and the second one was encapsulated. Asymmetric design allowed to actuate the flow in definite direction. When AC voltage of sufficient frequency and amplitude was applied the plasma region originated above the encapsulated electrode.

In experiment the sinusoidal voltage up to 7 kV with frequency 8.5-17.5 kHz was used. This allowed to reach a power in plasma of about 50-100 W or 330-670 W/m (length of the electrodes was 150 mm).

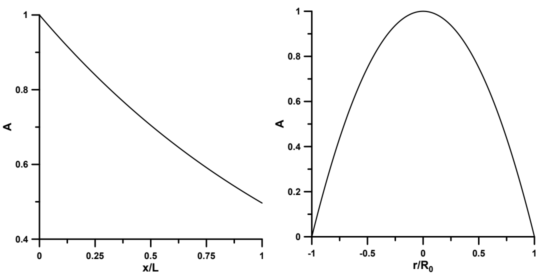

a b

Fig. 4. Shape of the streamers discharge (a – axial, b – radial).

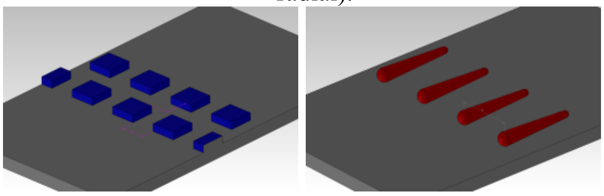

a b

Fig. 5. Type of disturbance (a – roughness, b – plasma).

Sufficient voltage potential between the electrode and dielectric surface must be provided for air breakdown in DBD. When this voltage potential achieved the local streamer generated, which transports a charge on (or from) the surface of the dielectric. This leads to a reduction the difference of potential and plasma off. Burning time of streamer depends on the parameters of discharge and in this experiment was approximately 100 ns. Accordingly, the formation of streamers is possible only when the voltage is alternating. For example, in this experiment the local discharge occurred at the same place approximately 5-7 times per period. Accordingly, the average frequency of a streamer was approximately 50 kHz (for the oscillator frequency of 8 kHz). Note that the time interval between the streamers is not fixed. It depends on the voltage gradient. For sinusoidal voltage plasma appears twice per the period in moments of maximum gradient. Generic feature of DBD is absence of a direct temporal phase coherence of streamers along the width of the discharge. It means that the appearing of streamers in classical burning of DBD for sinusoidal voltage is chaotic.

Nevertheless pulsations of the volume force generated by ion wind have good repeatability and their frequency equal to the frequency of high voltage generator [8].

Three main effects may be separated in the DBD action on the flow: 1) the local energy deposition in streamer heats the air and produces shock waves; 2) unsteady and non-uniform heating leads to deformation of the profile of the laminar boundary layer; 3) DBD induces the unsteady ionic wind. The impact of these factors may cause the boundary layer turbulization.

Table 1. Plasma parameters

<table>
<tr><th>F, kHz</th><th>P, W/m</th><th>M_∞</th><th>Re_1, m^{-1}</th><th>δ_0, mm</th><th>Re_{kk}</th><th>P_f, W/m</th><th>P/P_f, %</th></tr>
<tr><td>30</td><td>750</td><td rowspan="12">2</td><td rowspan="12">$10.1\cdot10^6$</td><td rowspan="12">0.534</td><td rowspan="8">5300</td><td rowspan="11">7870</td><td>9.5</td></tr>
<tr><td rowspan="5">50</td><td>810</td><td>10.3</td></tr>
<tr><td>1100</td><td>14.0</td></tr>
<tr><td>1250</td><td>15.9</td></tr>
<tr><td>1400</td><td>17.8</td></tr>
<tr><td>2140</td><td>27.2</td></tr>
<tr><td>70</td><td>1250</td><td>15.9</td></tr>
<tr><td>70</td><td>1750</td><td>22.2</td></tr>
<tr><td rowspan="3">50</td><td>950</td><td rowspan="3">1040</td><td>12.1</td></tr>
<tr><td>1600</td><td>20.3</td></tr>
<tr><td>400</td><td>5.1</td></tr>
<tr><td>-</td><td>1250</td><td>5300</td><td>7870</td><td>15.9</td></tr>
<tr><td rowspan="6">50</td><td>1250</td><td rowspan="6">1.5</td><td>$6.9\cdot10^6$</td><td>0.537</td><td>4050</td><td>7500</td><td>16.7</td></tr>
<tr><td>1250</td><td rowspan="5">$10.5\cdot10^6$</td><td rowspan="5">0.457</td><td>7420</td><td rowspan="5">9800</td><td>12.8</td></tr>
<tr><td>970</td><td rowspan="4">5700</td><td>9.9</td></tr>
<tr><td>1620</td><td>16.5</td></tr>
<tr><td>2140</td><td>21.8</td></tr>
<tr><td>2580</td><td>26.3</td></tr>
</table>

The advantage of CFD simulation is a possibility to separate DBD influences on the flow and to compare their effects. Two influence mechanisms were considered: 1) The single streamer was modeled by local energy deposition near the wall; 2) The ionic wind was modeled by addition of periodic volume force in the near-wall region.

Parameters of the volume force (frequency, amplitude) were taken from an experiment performed in quiescent air at pressures appropriate to the static pressure in the wind tunnel flow.

For the simulation of the heat source, the following assumptions were applied (close to the experiment):

1) The streamers frequency is constant.
2) Ignition of all streamers is synchronous.
3) The discharge streamer is a cylindrical region with the energy distribution shown in the figure 4. These parameters were chosen based on photographs of the discharge. For most calculations the cylinder length was 3 mm, radius 0.25 mm, and the distance between streamers 2 mm.
4) The duration of the volume heat source was 100 ns.
5) The average power of the heat source in the calculation was taken close to the experimental values.

DBD plasma excites significant disturbances in the flow therefore the process of boundary layer transition was simulated by LES approach with Smagorinsky subgrid model. The computation domain was meshed to provide $\Delta y+\approx 1$, $\Delta x+\approx 10$, $\Delta z+\approx 10$. Number of cells: ≈14 mil. Size of calculation area: 100x13x8 mm (Fig. 3). Boundary conditions correspond to experiment. Lines in the figure 3 indicate the profiles where the data were accumulated.

The calculation was performed by commercial CFD Fluent. The disadvantage of Fluent is low order of numerical scheme, so achieving of good accuracy requires a large grid. However, the low order of scheme makes it easy to avoid incorrect solutions in area of large gradients (like this problem).

In Table 1 one can find the parameters of the calculation with the DBD treated as volume heat source. Calculations were performed for the flow parameters close to experimental ones for M = 2 and planned experiments for M = 1.5. Boundary layer thickness is given in the zone of discharge. Re_{kk} parameter is taken from [9] and equals

$$Re_{kk} = \left.\frac{dU}{dy}\right|_{wall} \cdot \frac{\rho_k}{\mu_k} k^2 \quad (1).$$

It is well known that the flow with roughness at the same Re_{kk} demonstrate similar processes of laminar-turbulent transition. It was decided to verify the applicability of this parameter for plasma sources. The value of k is equal to the upper boundary of the plasma region. Power P - corresponds to the power of the plasma per unit length of the electrode. Power P_f - corresponds to the flow power in the boundary layer calculated as

$$P_f = c_p T_0 \cdot \rho U \cdot \left(\delta_0 - \delta_0^*\right) \quad (2).$$

The effect of plasma discharge on the flow was compared with effect of the roughness turbulator (base case). Zig-zag roughness with steps of 1 mm and a rectangular shape with a height of 0.3 mm were used.

3 Experimental and numerical results

Figure 6 shows an example of the artificial turbulization by DBD for M = 2 and $Re_1=10.5\text{-}10^6$ m^{-1}. The ionic wind was directed upstream in this case. The sandpaper turbulator was placed 70 mm downstream of the plasma actuator to obtain the turbulent boundary on the model if plasma is off. Figure 6 shows the effect of plasma on the boundary layer profiles measured by hot-wire anemometer. Activation of plasma results in growing of the boundary layer associated with upstream shifting the transition location. It can be seen that pulsation distribution across the boundary layer remains similar.

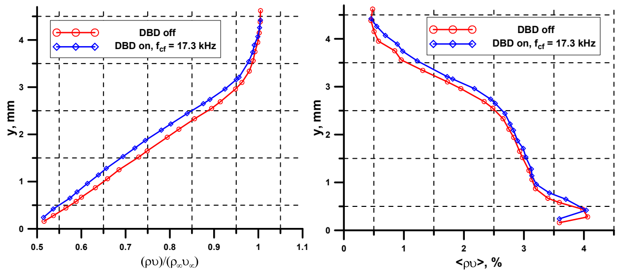

Fig. 6. Vertical profiles of mass flow and mass flow pulsations (RMS values) in the turbulent boundary layer (x = 260 mm)

These experiments revealed the possibility of using plasma discharge for turbulization of supersonic boundary layers but mechanisms of turbulization remained unclear. CFD simulation was performed to understand the mechanism from calculation results.

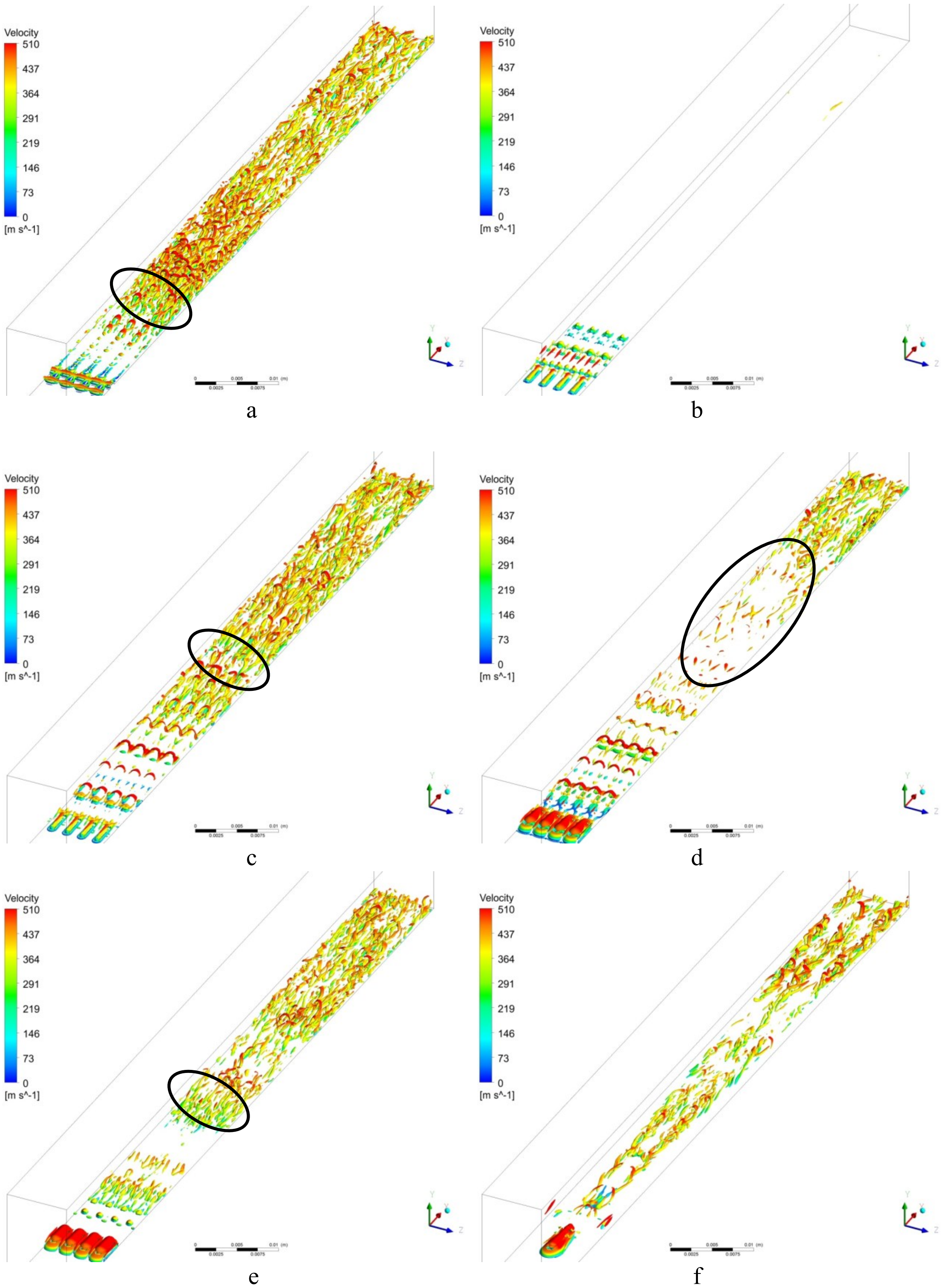

Fig. 7. Q-criterion (a – roughness, b – F = 50 kHz, W=810 W/m, c – F = 50 kHz, W=1250 W/m, d – F = 50 kHz, W=1400 W/m, e – F = 30 kHz, W=750 W/m, f – Single discharge W=400 W/m)

The first simulation did not show any significant influence of the ion wind on BL. Even an increase of the amplitude of the volume force by 10 times in comparison with the experiments did not allow to trigger rapid laminar-turbulent transition in the boundary layer. Therefore we will focus on the results obtained with volume heat sources.

In fig. 7. Q-criterion is used to visualize the introduction of perturbations and laminar-turbulent transition processes obtained for M = 2. It is clearly seen the rapid boundary layer turbulization for classical roughness. Downstream of the roughness the periodic structures are formed which quickly lose symmetry and lead to the chaotic turbulence in BL. Perturbations introduced by the discharge with low power (*P* = 810 W/m, fig. 7 b) decay rapidly and do not lead to turbulence. Increasing of the discharge power allows to achieve laminar-turbulent transition in the computational domain. Further increasing of energy from *P* = 1100 W/m to *P* = 1250 W/m shifts the position of the laminar-turbulent transition upstream. However if the power is equal to *P* = 1400 W/m the flow pattern considerably changes. The position of the symmetry breaking of periodic structures occurs approximately at the same coordinates X as for the case with power P = 1250 W/m, but downstream there is a long region with a non-equilibrium turbulent boundary layer. Further increasing of power results in growth of the initial periodic structures but their breakdown is delayed, and non-equilibrium boundary layer is formed.

Increase of the discharge frequency from 50 to 70 kHz (with different power) led to prevention of transition and laminar flow was kept throughout the whole computational domain. The same results were obtained for steady energy supply. In paper [10] it was shown that the steady energy supply generates a pseudo semi-infinite body, which does not lead to laminar-turbulent transition.

Increasing of frequency up to 70 kHz is similar to a quasi-stationary case, because thermal spots formed in discharge streamers have not enough time to leave the zone of energy supply before the next heating cycle.

Reducing of the frequency led to successful turbulization of flow (fig. 7 e) for lower average power (power of single streamer was the same as in the case presented in fig. 7 c). Moreover average discharge power necessary for quick tubulization of BL can be reduced by optimizing the distance between the streamers.

In fig. 7 f an example of calculation obtained for single heat source in the computational domain is shown. Successful turbulization of the flow can be seen for *P* = 400 W/m. But the end of the laminar-turbulent transition occurs significantly downstream.

Calculations performed for smaller radius of discharge (less Re_{kk}) showed more efficient generation of periodic structures. This means that the major role in introduction of the perturbation belongs to a gradient generated by heat source whereas the size of energy supply zone and absolute power are secondary parameters. Moreover the calculations for different distances from the wall to the center of heat supply were performed. The highest efficiency is achieved when the center of the discharge zone was near the critical layer. But creation of such a discharge in the experiment is very difficult.

In fig.8 one can see distribution of the boundary layer thickness the along the plate. The base case shows that a sharp increase of thickness occurs at a distance 20 mm from the roughness due to laminar-turbulent transition. In the case of steady heat supply or low power of DBD the boundary layer remains laminar. However in the case of unsteady energy supply there is increasing of the laminar boundary layer thickness.

Increasing of the discharge power results in increase of fluid displacement in the region of the discharge. Downstream the convective mixing of turbulent BL equalizes temperature and the difference between the thickness of the BL decreases. The roughness case has a good agreement with the logarithmic law and the distribution of Klebanoff (fig.9-10). The differences are due to the coarse mesh.

Preliminary calculations allowed to achieve a better agreement with a logarithmic law, but required a significantly larger grid, which greatly increased the computation time. Because the goal of this paper is a parametric study, and it requires a lot of time, it was decided to use a moderate grid. Therefore, the results of the plasma will be compared to the base case (roughness).

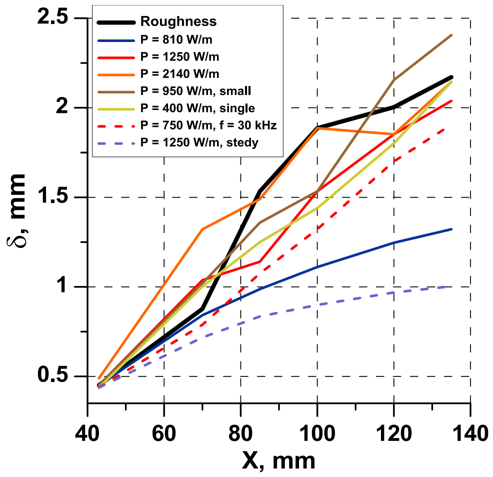

Fig. 8. Thickness of boundary layer at M=2

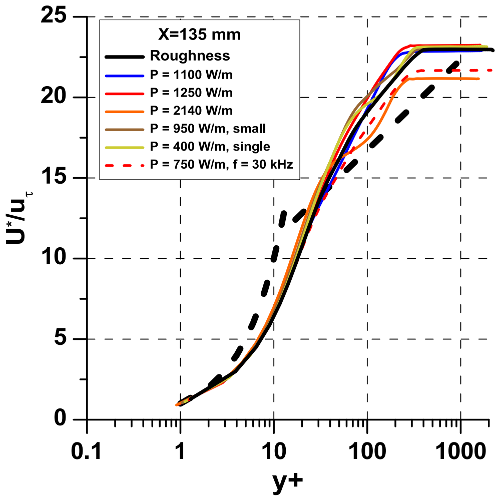

Fig. 9. Mean velocity profile at M=2

It is clearly seen that for low or high plasma power there are large differences compared to the base case. Most probably that for low power of discharge the process of laminar-turbulent transition is not yet complete. At high power boundary layer becomes non-equilibrium due to the influence of thermal wake. However with increasing distance from the zone of initial perturbation this difference decreases. This is clearly seen in Fig. 12. The behavior of the turbulent flow in the case of roughness and plasma source are qualitatively the same.

The powerful heat source generates large-scale structures. These structures are not destroyed for a long time. The flow “remembers” the wake from the powerful heat input until the end of the computational domain. This may lead to delay of laminar-turbulent transition. The zones of thermal wake have low speed, it reduces the boundary layer resistance to adverse pressure gradient and therefore they should be avoided.

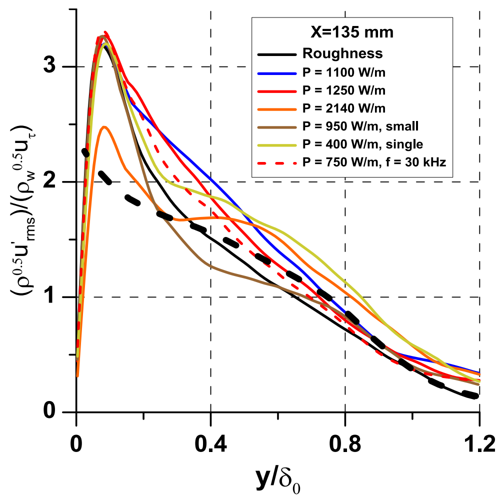

Fig. 10. Turbulence distribution at M=2

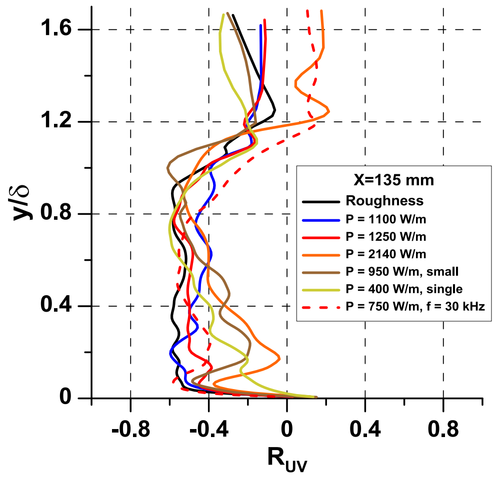

Fig. 11. Correlation coefficients between longitudinal and normal velocity at M=2

Distribution of correlation coefficients confirm the achievement of nearly equilibrium turbulent boundary layer (fig. 11). But some distortion can be seen near the wall due to the presence of the thermal wake for a powerful source.

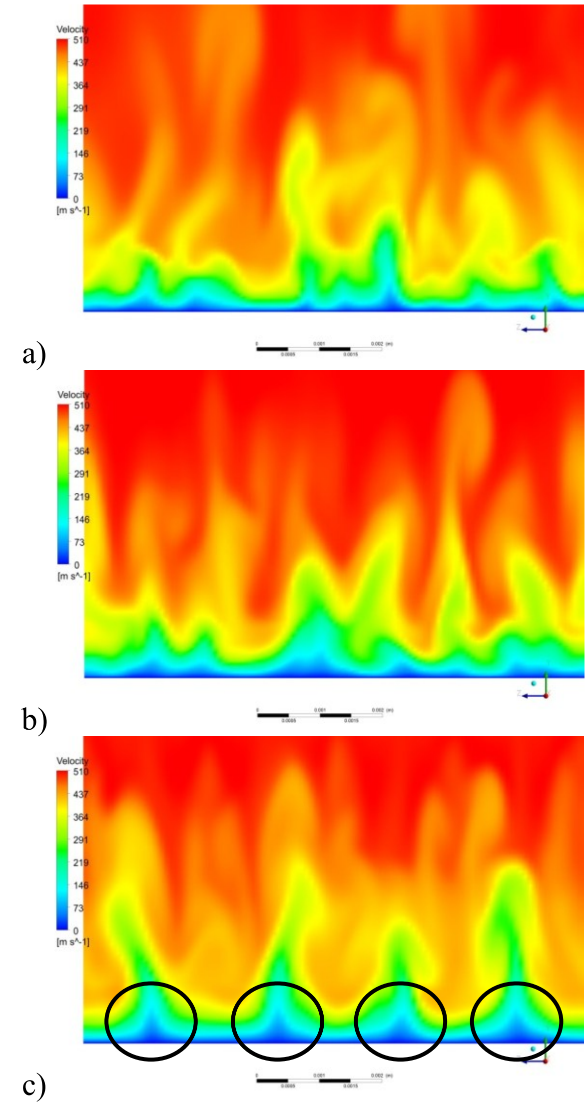

Fig. 12. Instantaneous velocity distribution in cross-section at X=125 mm (a – roughness, b – W=1250 W/m, c – W=2140 W/m)

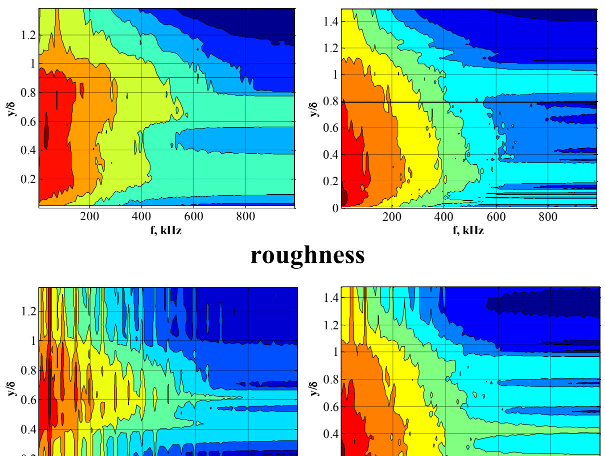

W=1250 W/m

X = 70 mm X = 135 mm

Fig. 13. Power spectra density of longitudinal velocity

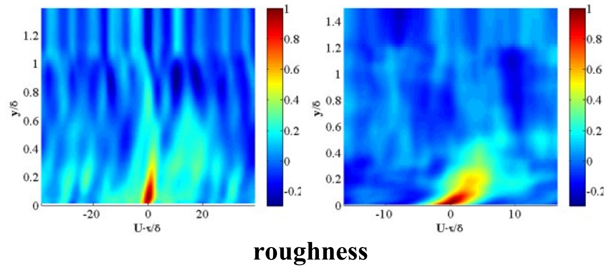

W=1250 W/m

X = 70 mm X = 135 mm

Fig. 14. Cross-correlation of velocity

Outside of the boundary layer correlation coefficients are different for the roughness and discharge cases. This is due to the periodic thermal perturbations in the case of discharge.

The most equilibrium boundary layer is achieved by the formation of strong disturbances at low energy supply (low heat source, the cases of F = 30 kHz and a small discharge).

In fig. 13 presence of the forcing frequency and its harmonics in the case of discharge in the section X = 70 mm can be seen. The spectrum inside the boundary layer becomes smooth downstream. At the end of the computation domain the spectrum for the case of the discharge is close to the spectrum in the case of roughness.

It is interesting to note that at the beginning of turbulization (X = 70 mm) spectra are similar (except the near-wall zone) despite the different mechanisms of introduction of the perturbations.

In fig. 14 shows cross-correlation between velocity pulsation near the wall not far from disturbance region (Y=0.04 mm, X=70 mm) and velocity at different profiles.

From cross-correlations can it be found, that roughness generates a periodic flow (vortex street), which is not found at the end of the computational domain.

a)

b)

c)

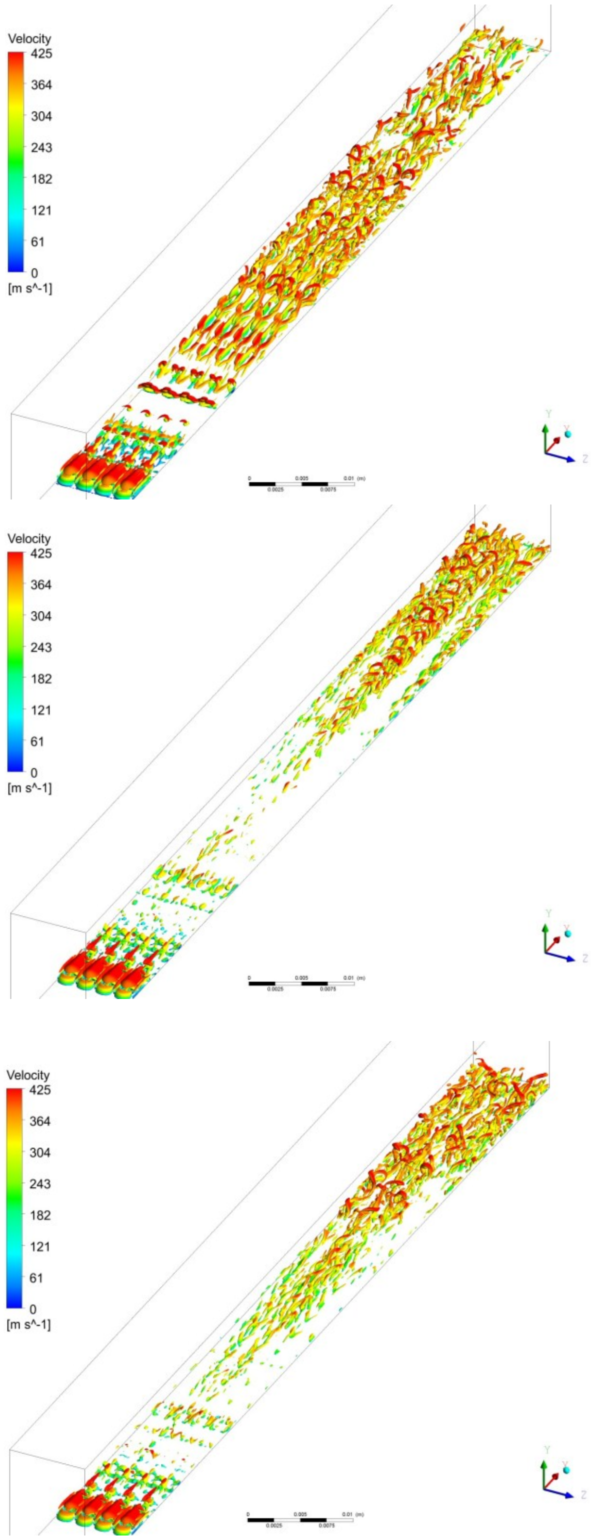

Fig. 15. Q-criterion (a – W=1250 W/m, Re_1=6.9·10^6 m^{-1}; b – W=1250 W/m, Re_1=10.5·10^6 m^{-1}; c – W=970 W/m, Re_1=10.5·10^6 m^{-1})

Discharge generates developed periodic flow. With the development of turbulence the influence of forcing disturbances on the flow reduces. This means that the flow forgets the mechanism leading to laminar-turbulent transition.

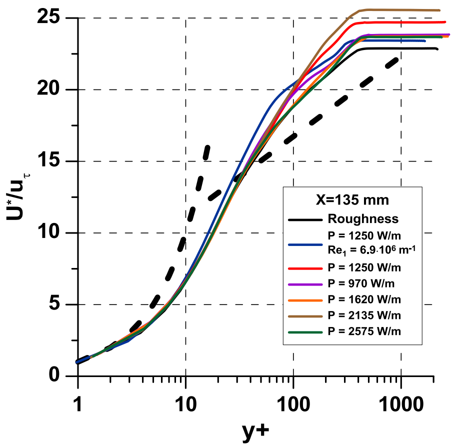

Fig. 16. Mean velocity profile at M=1.5

Calculations for M = 1.5 were performed at Re_{kk} close to the parameters M = 2 test case. Moreover the effect of variation of Re_{kk} at the same power density was studied (Fig. 15).

Qualitative flow pattern of perturbation (Q-criterion) for M = 1.5 is not different from M = 2. In the figure it can be seen that at low unit Reynolds number (small Re_{kk}) a good qualitative agreement with M = 2 (obtained for the same power) was obtained. Most probably this is due to similar levels of power ratio P/P_f for this Reynolds number. But Fig. 16 shows that in contrast to M = 2 the equilibrium turbulent boundary layer at the end of computational domain was not achieved. When a unit Reynolds number increases (density increases) the transition shifted downstream (Fig. 15 b, c). This can be explained by decrease of power ratio P/P_f (due to increase of density). But it already was noted that the discharge power is not a good criterion of the effectiveness of perturbation excitation. More important parameter is the spatial gradient of the flow parameters generated by the plasma. Therefore, reducing the diameter of the discharge (Fig. 15 c) allowed to shift position of the laminar-turbulent transition upstream.

Increasing of the discharge power for fixed Re_{kk} demonstrates the gradual approach of the BL to the base case (roughness). However, even high power deposition ($P/P_f > 20\%$) does not result in non-equilibrium BL due to the thermal effect, in contrast to the calculations carried out for M = 2. This can be explained by the imperfection of the dimensionless parameters used in this paper. This means that for plasma laminar-turbulent transition control optimization it is necessary to develop a dimensionless parameter taking into account features the discharge.

4 Conclusions

In paper the possibility of DBD application for turbulization of BL was confirmed experimentally and numerically. Calculations showed that the ionic wind (at this moment) cannot lead to quick laminar-turbulent transition. It was found that the main effect occurs due to heat generation in streamers namely formation of thermal spots and shock waves in BL. This creates a powerful periodic structures which lead to turbulization of BL.

Significant influence of thermal wake on the development of turbulence was found. It was shown that the best effect may be obtained for generation of heat perturbations with high gradient of energy but a small level of power.

This study was supported by Russian Science Foundation, grant 14-11-00490.

References

[1] E. Allison, I. Kroo, P. Sturdza, Y. Suzuki, H. Martins-Rivas. Aircraft Conceptual Design With Natural Laminar Flow. *27th International Congress of the Aeronautical Sciences*, 2010.

[2] M. Swoboda and W. Nitschef. Shock Boundary-Layer Interaction on Transonic Airfoils for Laminar and Turbulent Flow. *Journal of aircraft*. Vol. 33, pp. 100-108, 1996.

[3] Joslin R.D. and Miller D. *Fundamentals and Applications of Modern Flow Control. Vol. 231*: Progress in Astronautics and Aeronautics Series. AIAA, Inc, 2009.

[4] N. De Tullio, P. Paredes, N. D. Sandham, and V. Theo. Laminar-turbulent transition induced by a discrete roughness element in a supersonic boundary layer. *J. Fluid Mech*. Vol. 735, pp. 613-646, 2013.

[5] E. Orlik, N. Lardjane, I. Fedioun. Numerical investigation of laminar-turbulent transition forced by wall injection in hypersonic boundary layers. *5th European Conference for Aeronautics and Space Sciences (EUCASS 2013)*. Munich, Germany. 2013.

[6] D. Roupassov, A. Nikipelov, M. Nudnova, A. Starikovskii. Flow Separation Control by Plasma Actuator with Nanosecond Pulsed-Periodic Discharge. *AIAA Journal*.Vol.47, No.1, pp. 168-185, 2009. doi: 10.2514/1.38113

[7] S. Im, H. Do and M. A. Cappelli. Dielectric barrier discharge control of a turbulent boundary layer in a supersonic flow. *Applied Physics Letters*. Vol. 97, 2010.

[8] P.A. Polivanov, O.I. Vishnyakov, A.A. Sidorenko, and A.A. Maslov. Investigation of a Nonstationary Flow Field Generated by a Dielectric Barrier Discharge. *Technical Physics*. Vol. 57, No. 4, pp. 457-467, 2012.

[9] G. Groskopf and M.J. Kloker. Abstract Effects of an oblique roughness on hypersonic boundary-layer transition. *High Performance Computing in Science and Engineering '12*. pp. 255-276, 2013.

[10] M.A. Keller, M.J. Kloker, S.V. Kirilovskiy, P.A. Polivanov , A.A. Sidorenko, A.A. Maslov. Study of flow control by localized volume heating in hypersonic boundary layers. *CEAS Space J*, 2014. P.14. DOI 10.1007/s12567-014-0064-y

5 Contact Email Address

Polivanov P.A. – polivanov@itam.nsc.ru
Sidorenko A.A. – sindr@itam.nsc.ru

Copyright Statement